A robust assay to measure DNA topology-dependent protein binding affinity

Tamara R. Litwin[1,2], Maria Solà[3], Ian J. Holt[4] and Keir C. Neuman[1,*]

[1]National Heart, Lung, and Blood Institute, National Institutes of Health, Bethesda, MD 20814, USA, [2]Mitochondrial Biology Unit, Medical Research Council, Wellcome Trust/MRC Building, Hills Road, Cambridge, CB2 0XY, UK, [3]Department of Structural Biology, Molecular Biology Institute of Barcelona (CSIC), 08028 Barcelona, Spain and [4]National Institute for Medical Research, Medical Research Council, The Ridgeway, Mill Hill, London, NW7 1AA, UK

ABSTRACT

DNA structure and topology pervasively influence aspects of DNA metabolism including replication, transcription and segregation. However, the effects of DNA topology on DNA-protein interactions have not been systematically explored due to limitations of standard affinity assays. We developed a method to measure protein binding affinity dependence on the topology (topological linking number) of supercoiled DNA. A defined range of DNA topoisomers at equilibrium with a DNA binding protein is separated into free and protein-bound DNA populations using standard nitrocellulose filter binding techniques. Electrophoretic separation and quantification of bound and free topoisomers combined with a simple normalization procedure provide the relative affinity of the protein for the DNA as a function of linking number. Employing this assay we measured topology-dependent DNA binding of a helicase, a type IB topoisomerase, a type IIA topoisomerase, a non-specific mitochondrial DNA binding protein and a type II restriction endonuclease. Most of the proteins preferentially bind negatively supercoiled DNA but the details of the topology-dependent affinity differ among proteins in ways that expose differences in their interactions with DNA. The topology-dependent binding assay provides a robust and easily implemented method to probe topological influences on DNA-protein interactions for a wide range of DNA binding proteins.

INTRODUCTION

Complex DNA topological states arise *in vivo* from a variety of cellular processes. Replication (1) and transcription (2) alter DNA topology by generating positive supercoils ahead of the polymerase and, for RNA polymerase, negative supercoils behind it. Both processes can fail if this torsion is not relieved (3). In addition, DNA replication on a torsionally constrained molecule leads to extensive precatenation (4,5) that, if left unresolved, can prevent effective segregation of the replicated chromosomes during the G2 phase of the cell cycle (6) and may lead to cell death. Recombination reactions and the action of topoisomerases can also lead to DNA knotting, a third form of topological variation (7).

In spite of the large energetic costs of doing so, DNA is maintained in a negatively supercoiled state *in vivo* in most organisms, likely in order to facilitate transcription and melting of the DNA duplex by proteins that need to access single-stranded DNA (8–10). Supercoiling also compacts DNA, facilitating efficient packaging in the nucleus or nucleoid (11). Furthermore, supercoiling increases the probability of the juxtaposition of two distal sites on DNA (12), potentially reducing the search time of enzymes that bind to a synapse of two such sites. Whereas historically DNA has been seen as a passive recipient of protein activities upon it, more recently it has been shown that the topological state of DNA can have regulatory effects, such as promoting transcription (13) and sequence specificity in otherwise non-specific proteins (14). Because supercoiling and other complex topological states are ubiquitous *in vivo*, DNA topology likely affects the majority if not all cellular process involving DNA. Therefore, it is important to consider the effects of topology on protein binding to DNA.

Whereas many biochemical and biophysical investigations use short linear DNA molecules that are necessarily topologically relaxed, this does not accurately represent the topologically constrained state of DNA *in vivo*. The fact that supercoiled DNA is in a higher energy state than relaxed DNA may make protein binding more favorable by reducing the energy required for any associated twisting or bending of the DNA (15). This suggests that traditional methods of determining binding association and dissociation constants, or K_a and K_d values, may provide an incomplete picture of DNA-protein interactions in the cell. When the effects of topology on binding are considered, measurements typically compare relaxed or nicked with highly su-

percoiled DNA, and measurements of topology-dependent binding at intermediate supercoiling values have not previously been quantified (16). Measuring and quantifying DNA-protein interactions for a defined range of topological forms of DNA will provide insight into the modulation of protein-nucleic acid interactions by DNA topology.

Electrophoretic mobility shift assays (EMSAs) are often used to determine binding affinity, but they can only be used with one DNA substrate at a time and the binding reaction is out of equilibrium, which limits the range of affinities that can be measured and may bias the results. In addition, EMSAs generally measure average binding to a Gaussian distribution of topoisomers. One solution to obtain sensitive, quantitative topology-dependent binding has been to isolate and measure the binding of individual topoisomers, but the inefficiency of the process has limited its use to no more than one or two topoisomers, and previous work generally compared two forms of DNA (17). Linear versus supercoiled DNA binding by Topo IV have also been compared (18). Filter binding assays have been used to measure topology-dependent protein binding (19,20). In these assays, enzyme binding to a radiolabeled linear DNA substrate was measured and the affinity for relaxed or highly negatively supercoiled DNA was estimated through competitive binding with the labeled linear DNA (19).

Here, we develop a topology-dependent binding assay that can determine the relative binding affinities of many topoisomers simultaneously. The substrate DNA spans a range of supercoiling densities and can be used with any protein that binds to nitrocellulose. Previous measurements adapted the standard filter binding approach by performing electrophoretic separation of the free and protein-bound DNA after elution from the nitrocellulose filter (16), providing a qualitative measure of the relative binding affinity to relaxed, nicked and highly supercoiled DNA but not quantifying protein binding to specific DNA topoisomers. We expanded upon this approach to create a topology-dependent binding assay that measures relative binding affinity as a function of DNA linking number (ΔLk) or supercoiling density (σ) though the quantification and normalization of the amount of each DNA topoisomer in the bound and free fractions. Detection with SYBR Green I stain results in high sensitivity, and the internal normalization inherent in the measurement makes the assay robust against uneven pipetting, gel loading, topology-dependent SYBR green staining efficiency and other errors that would affect absolute affinity measurements. In addition, the binding is assayed under equilibrium conditions, an improvement over EMSA methods, which, strictly speaking, are out of equilibrium. Finally, the nitrocellulose filter binding experiments are carried out under conditions that minimize the probability of multiple protein binding, eliminating the complications associated with standard filter binding assays for which the interpretation depends on models of multiple protein binding (21).

We tested the topology-dependent DNA binding affinity of a variety of DNA binding proteins including the mitochondrial transcription factor Tfam, the type II restriction endonuclease EcoRV, the prokaryotic DNA helicase RecQ, catalytic mutants of human nuclear and mitochondrial topoisomerase IB and wild-type and a catalytic mutant of the prokaryotic type IIA topoisomerase IV (Topo IV). These proteins were selected to represent several classes of DNA binding proteins. The topology-dependent binding properties of a subset of these proteins could be compared with published estimates. With the exception of the sequence-specific protein EcoRV, each protein displayed topology-dependent affinity changes that highlight the importance of topology in DNA-protein interactions.

MATERIALS AND METHODS

Reagents and materials

Reagents. Chemicals were purchased from Sigma-Aldrich (St. Louis, MO, USA) unless otherwise noted.

Proteins. The restriction endonuclease EcoRV (20 000 U/ml) was purchased from NEB. The activity of EcoRV in the supplier-provided buffer was verified by completely linearizing plasmid DNA containing a single EcoRV site (data not shown). Human nuclear Topoisomerase I (ntop1) with an active site mutation (Y723F) was purchased from TopoGEN. Human mitochondrial topoisomerase I (top1mt) with an active site mutation (Y559F) was a generous gift of Dr. Yves Pommier of the National Cancer Institute. Human Tfam containing a his-tag and lacking the mitochondrial targeting sequence was purified as previously described (22). TEV was also purified as previously described (23). *Escherichia coli* RecQ was a generous gift from Dr. Marie-Paule Strub of the National Heart, Lung, and Blood Institute.

E. coli Topo IV wild-type subunits, ParC and ParE, and the active site mutant, ParC Y120F, were purified from *E. coli* BL21-CodonPlus(DE3)-RIL cells as described in (24) and (25). Briefly, protein overexpression was induced by adding 0.5 mM IPTG and incubating at 37°C for 4 h. The cells were harvested by centrifugation and frozen at −80°C. For each purification, 1.5 g of frozen cells were thawed and resuspended in 25 ml Buffer A (20 mM HEPES pH 7.5, 800 mM sodium chloride (NaCl), 10 mM imidazole, 2 mM β-mercaptoethanol (βME) and 10% glycerol) supplemented with 1× protease inhibitor cocktail (Roche) and 100 μg/ml lysozyme. The cells were lysed with an EmulsiFlex-C3 emulsifier (Avestin). The cell lysate was centrifuged at 9000 revolutions per minute (rpm) at 4°C for 30 min to pellet large cell debris. The supernatant was centrifuged again at 40 000 rpm at 4°C in a Beckman XL-100 centrifuge. The supernatant was loaded on a Ni-NTA Superflow Column (Qiagen) previously equilibrated with Buffer A. Buffer A and Buffer B (20 mM HEPES pH 7.5, 800 mM NaCl, 1 M imidazole, 2 mM βME and 10% glycerol) levels were adjusted to create a linear gradient from 10 to 800 nM imidazole while collecting 2 ml fractions. Fractions encompassing the major protein peak were checked for purity using tris-glycine gels (Invitrogen), then pooled and concentrated to a volume of ~1 ml using an Amicon Ultra-15 Centrifugal Filter Unit with 50 kDa molecular weight cutoff (Millipore) at 4°C. The his-tag was cleaved by adding a 1:100 $OD_{280 \text{ nm}}$ ratio of TEV protease: Par protein and incubating at 4°C overnight. TEV-cleaved ParE or ParC subunits were run over a Superdex 200 10/300 GL column (GE Healthcare) in gel filtration buffer (20 mM HEPES pH 7.5, 400 mM NaCl, 2 mM βME and 10% glycerol) while collecting 2 ml fractions. The

fractions comprising the center of the peak were checked for purity by polyacrylamide gel electrophoresis gel. The mass of each purified protein was confirmed by mass spectrometry and the final concentration was determined from the absorbance using extinction coefficients ϵ = 57 300 for ParC and ϵ = 67 840 for parE. ParC and ParE were combined in a 1:1 molar ratio and stored at $-80°$C. ParC Y120F was stored at $-80°$C and combined with wild-type ParE in a 1:1 molar ratio immediately prior to use.

Preparation of extended topoisomer distribution

E. coli DH5α cells were transformed with pBR322 (NEB) and grown to mid log phase in LB broth while shaking at 37°C. Plasmid was purified from the cells using a Qiagen maxi prep kit. This plasmid was used without further purification for experiments with supercoiled DNA. An extended DNA topoisomer distribution for all other binding experiments was made by partially relaxing supercoiled pBR322 with Topo IV. Note that 100 µg pBR322 was diluted in 1 ml Topo IV buffer supplemented with 1 mM adenosine triphosphate (ATP). Topo IV was added to a final concentration of 7 nM of the assembled heterotetramer and the reaction was allowed to proceed at room temperature for 90 s and then quenched with one volume of isopropanol. The precipitated DNA was washed with 70% ethanol and resuspended in 10 nM Tris pH 7.5. The topoisomer distribution was checked by agarose gel electrophoresis. Partially relaxed DNA visualized after electrophoresis in chloroquine-containing gels suggested that very little positively supercoiled DNA was generated in the reaction (data not shown). Residual ATP was removed by adding 100 mU apyrase (NEB) to the DNA in Topo IV buffer supplemented with an additional 10 mM MgCl$_2$for 1 h at 37°C before repeating the precipitation step (as above) to remove the apyrase enzyme.

Topology-dependent binding assay

Binding reaction conditions. Under the assumption of random, non-cooperative binding, the number of proteins bound per DNA will follow a Poisson distribution. Under these assumptions, DNA and protein concentrations were adjusted based on published K_d values to ensure that less than 5% of DNA molecules would be expected to have greater than one protein bound. Establishing this condition simplifies analysis of the filter binding results since each bound DNA can be assumed to be bound to a single protein, rather than multiple proteins.

Binding reactions for all proteins were in 0.5 ml total volume. EcoRV binding reactions contained 2.5 nM EcoRV and 5 nM pBR322 in 100 mM NaCl, 50 mM Tris-HCl pH 7.5 and 10 mM calcium acetate. Adding calcium to the buffer while omitting magnesium allows EcoRV to bind to but not cleave the DNA (26). Tfam binding reactions contained 10 nM Tfam and 10 nM pBR322 in 150 mM NaCl, 10 mM Tris pH 7.5, 10 nM MgCl$_2$ and 1 mM DTT based on the buffer conditions used in (27). Topo IV binding reactions for both the wild type and Y120F constructs contained 2 nM Topo IV and 10 nM pBR322 in 40 mM Tris-HCl pH 7.5, 6 mM MgCl$_2$, 100 mM potassium acetate,

1 mM DTT and 0.1 mM ethylenediaminetetraacetic acid (EDTA). Omitting ATP from the buffer allows wild-type Topo IV to bind to DNA but not complete strand passage events. RecQ binding reactions contained 10 nM pBR322 and 50 nM RecQ in 50 mM Tris, 50 mM NaCl, 5 mM MgCl$_2$ and 1 mM DTT. The absence of ATP forestalled the possible topological complications of helicase activity. Topo IB binding reactions contained 10 nM pBR322 and 10 nM ntop1 Y723F or top1mt Y559F in 10 mM Tris-HCl pH 8.0, 50 mM KCl, 10 mM MgCl$_2$, 0.1 mM EDTA and 5 mM DTT. The tyrosine to phenylalanine mutation in the DNA-cleavage domain of Topo I prevents supercoil relaxation.

Separation of bound from unbound DNA. After allowing the binding reactions to equilibrate for 30 min to 1 h at 37°C, the protein-DNA mixture was loaded onto a 0.45 µm nitrocellulose Centrex MF filter (Whatman) pre-washed with the binding buffer of the relevant protein. The eluate, containing unbound DNA, was collected by centrifuging for 5 min at 2000 rpm. The column was washed by repeating the centrifugation after adding 1 ml binding buffer. Finally, the protein-bound DNA retained in the column was eluted by adding 0.1% sodium dodecyl sulphate (SDS) solution.

DNA preparation and agarose gel conditions. Bound and unbound DNA fractions were concentrated to ∼30 µl using 30 kDa Amicon Ultra-0.5 columns (Millipore) pre-washed with 10 mM Tris pH 7.5. The fractions were resuspended in 10 mM Tris pH 7.5 and concentrated again to exchange the buffer before eluting them by centrifuging the filter columns upside down in a collection tube. The DNA was quantified with a Nanodrop-1000 (Thermo) before loading 30 ng of DNA in each lane of a 1% agarose gel in TAE and running at 2.5 V/cm for 16–18 h at 4°C. Gels containing highly supercoiled pBR322 were electrophoresed with 3.5 µg/ml chloroquine present in both the gel and the buffer, and the chloroquine-containing gels were destained by washing five times for 20 min in 250 ml water. Gels free of chloroquine or after chloroquine removal were stained with 1$\times$ SYBR Green I (Life Technologies) for 40 min at 4°C and imaged using a Biospectrum AC Imaging System equipped with a Chemi 410 2MP CCD camera (UVP).

Data extraction and fitting. ImageJ 1.46 was used to extract the data as intensity per pixel from the CCD images of the agarose gels. Images were background corrected using a rolling circle method with a circle size of between 50 and 100 pixels. Igor Pro 6 (Wavemetrics) was used for subsequent curve fitting, analysis and data visualization. A serial dilution of DNA was used to ensure that SYBR green gives a linear response across the range of DNA concentrations used for the topology-dependent binding assay and that the CCD response was linear over this range of intensities (data not shown).

RESULTS

Development of a DNA topology-dependent binding assay

To determine the relative affinities of DNA binding proteins for DNA topoisomers ranging from relaxed to super-

coiled with a supercoiling density of -6% ($\sigma = -0.06$), we combined the separation of free from protein-bound DNA by nitrocellulose filter binding with the separation of DNA topoisomers in each fraction by agarose gel electrophoresis. The relative topoisomer amounts in bound and unbound fractions could then be quantified. Briefly, a solution containing a range of DNA topoisomers generated by a partial relaxation reaction with Topo IV (see Materials and Methods) was allowed to equilibrate in the presence of a DNA binding protein. The solution was run over a nitrocellulose column to separate protein bound from unbound DNA molecules. The topoisomers of the bound and unbound DNA fractions were separated by agarose gel electrophoresis (Figure 1). Finally, after staining, the gel was imaged and the relative amounts of bound and unbound topoisomers were quantified by Gaussian fitting of the distribution of intensity values of each band. The relative K_a values for each topoisomer were calculated from the ratios of the bound and unbound fractions normalized by the ratio of a given topoisomer. The shape of the binding affinity distribution is insensitive to the choice of normalizing topoisomer, but for clarity and to facilitate comparisons among proteins, the fully relaxed closed circular form ($\Delta L_k = 0$) was typically used with exceptions as noted. Approximately 10 distinct topoisomers could be resolved in each gel, with topoisomers for values of ΔL_k below -10 unresolvable. A single Gaussian was fit to these clustered bands, which were assigned a value of $\Delta L_k = -23$ based on an estimate of their expected topoisomer value.

The activity of several of the tested proteins alters the topology of DNA. For instance, Topo IV and Topo IB relax DNA from supercoiled states. EcoRV linearizes DNA, and RecQ unwinds it. In each instance information about the state of the bound protein–DNA complex is lost if the reaction is allowed to proceed. Therefore, binding affinity measurements were performed under conditions that permit binding but inhibit activity. Topo IV and RecQ binding measurements were performed in the absence of ATP, which is required for activity but not for binding. EcoRV binding reactions were performed in a buffer containing calcium in place of magnesium, which inhibits cleavage but not binding (28). Topo IB binding and activity are difficult to uncouple, so mutant nuclear and mitochondrial Topo IB enzymes with a tyrosine to phenylalanine mutation in the active site that can bind to but not cleave DNA were used (29). Tfam does not alter DNA linking number so binding measurements were made in standard Tfam buffers.

Analysis of relative DNA binding affinity

The association constant K_a for any topoisomer i in solution is defined by the formula in Equation (1), where $[E]$ is the concentration of the free enzyme, $[D_i]$ is the concentration of the free ith topoisomer and $[ED_i]$ is the concentration of the enzyme bound ith topoisomer

$$Ka_i = \frac{[ED_i]}{[E][D_i]} \tag{1}$$

The ratio of K_a values for two topoisomers i and j in equilibrium in solution is determined by dividing the K_a equations for each topoisomer (Equation 2)

$$\frac{Ka_j}{Ka_i} = \frac{[E][D_i]}{[ED_i]} * \frac{[ED_i]}{[E][D_j]} \tag{2}$$

Because the concentration of free enzyme $[E]$ is the same for all topoisomers in a solution at equilibrium, it drops out of the equation (Equation 3). After eliminating the enzyme concentration from the equation it becomes apparent that the relative K_a values for topoisomers can be determined solely from the ratios of the concentrations of unbound DNA ($[D_i]/[D_j]$) and of enzyme-bound DNA ($[ED_j]/[ED_i]$)

$$\frac{Ka_j}{Ka_i} = \frac{[D_i][ED_j]}{[D_j][ED_i]} \tag{3}$$

The relative concentrations of the topoisomers were determined by densitometry of digital images of agarose gels post-stained with SYBR green. Intensity profiles of each lane were background corrected and fit to a sum of Gaussians (Figure 2). The ratio of the areas of any two peaks provides the desired ratios of unbound topoisomers ($[D_i]/[D_j]$) and enzyme-bound topoisomers ($[ED_j]/[ED_i]$). Since this calculation relies entirely upon ratios, systemic errors or variations in gel loading due to pipetting errors cancel out when the ratio of K_a values is calculated. Similarly, differences in SYBR Green staining efficiency of different DNA topoisomers that would otherwise complicate the analysis (30) cancel out when the K_a ratio is computed (Equation 3).

Topo IV–DNA binding is strongly topology-dependent

The *E. coli* type IIA topoisomerase Topo IV binds highly negatively supercoiled DNA ($\sigma = -0.06$; $\Delta L_k = -25$ for pBR322) with ~5-fold higher affinity than relaxed circular DNA (31). However, the affinity for intermediate topoisomers has not been determined. We reasoned that the affinity of Topo IV likely depends on the topology for intermediate values of supercoiling and thus would be a good test case for the method we developed. After background correction of the agarose gel images, the intensity as a function of position along each lane was extracted (Figure 2A and B). Highly supercoiled DNA makes up a higher proportion of the bound DNA population, while relaxed and open circular (nicked) DNA make up a higher proportion of the unbound DNA population. A Gaussian distribution was fit to each peak and the area of the peak was taken as a measure of the amount of DNA in the band. The relative K_a values for each topoisomer were calculated using Equation (3), normalized to the first distinguishable topoisomer ($\Delta L_k = -1$) (Figure 2C).

Topo IV had ~5-fold higher affinity for 6% negatively supercoiled DNA than for fully relaxed DNA, consistent with previous measurements (31). K_a values for Topo IV increased monotonically with the absolute value of the linking number (Figure 2C). The experiment was repeated with a Topo IV in which the active site tyrosine was mutated to a phenylalanine (Y120F) that prevented cleavage of the DNA. The resulting binding profile is not as linear as that of wild-type Topo IV (Figure 2C). At low values of the linking number the relative affinity is decreased, whereas it is increased for highly supercoiled DNA (Figure 2C). It is some-
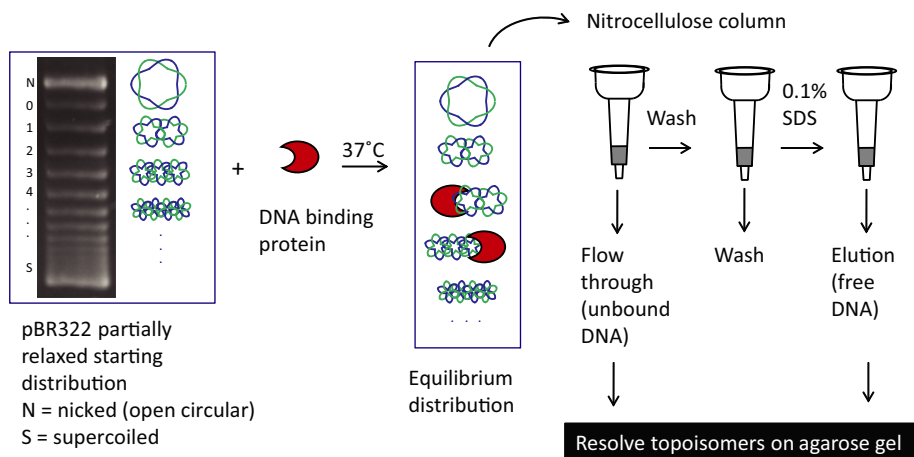
Figure 1. Topology-dependent binding assay. A DNA binding protein is added to a distribution of DNA topoisomers and allowed to equilibrate. The reaction is passed through a nitrocellulose filter, trapping the protein and protein-bound DNA while allowing free DNA to flow through. After washing with binding buffer, 0.1% SDS is used to elute the protein-bound DNA from the column. The unbound and bound DNA distributions are compared on an agarose gel.

what surprising that mutation of the active site tyrosine results in such a large difference in the binding affinity profile. Since the DNA is cleaved in only 8% of Topo IV-DNA complexes at any given time in the absence of ATP (32), elimination of cleavage by mutation of the active site tyrosine would have a modest effect on the measured binding affinity even if there was a substantial difference in affinity for cleaved and intact DNA. Consistent with this, we did not observe the formation of linearized plasmid in the agarose gels after Topo IV binding reactions, suggesting that the percentage of cleavage complexes is undetectably low. Since the Y120F alters the DNA binding pocket in addition to eliminating DNA cleavage, it is possible that the differences in topology-dependent binding reflect more fundamental structural effects (33).

Comparison of topology-dependent affinity for different classes of DNA binding proteins

We next measured the topology-dependent affinity of several different DNA binding proteins to determine if there are commonalities among different classes of enzymes. We tested catalytic mutants of two type IB topoisomerases (human nuclear topoisomerase IB, ntop1; and human mitochondrial topoisomerase IB, top1mt), a prokaryotic helicase (RecQ), a restriction endonuclease (EcoRV) and a mitochondrial transcription factor (Tfam) (Figure 3A). In general, the proteins displayed higher or equal binding affinity for negatively supercoiled compared to relaxed DNA, but the degree of topology-dependent binding varied among the proteins (Figure 3A).

Nuclear topoisomerase I (ntop1) displayed a moderate preference for supercoiled DNA but a very strong preference for binding to nicked DNA ($K_{\text{a\_Nicked}}/K_{\text{a\_Relaxed}} = 8.6 \pm 3.3$; Figure 3B). Type IB topoisomerases cleave a single strand of DNA (34) and have been shown to bind nicked DNA with high affinity (35). The lack of a binding preference for supercoiled DNA is surprising in light of previously reported strong binding preference for supercoiled DNA

(16,36). Repeating the experiment with the catalytic mutant of top1mt, the core domain of which is 73% identical and 87% similar to ntop1 (37), gave nearly identical results (Figure 3A). Previous measurements of Topoisomerase I binding were performed under conditions of excess protein, circumstances under which vaccinia topoisomerase IB binding has been shown to be cooperative (38). It is possible that similar cooperative binding may have affected the results of previous measurements.

RecQ exhibited a high degree of topology-dependent binding with a clear preference for negatively supercoiled DNA. If the helicase needs to intercalate into the double helix to unwind DNA, it may benefit energetically from the less tightly wound forms present in negatively supercoiled DNA.

The pBR322 substrate contained one EcoRV recognition sequence, so at most one EcoRV would bind with high affinity to each plasmid. EcoRV binding affinity was almost independent of DNA topology, likely reflecting that fact that EcoRV binding is sequence specific. EcoRV could also be expected to have higher sensitivity to the presence of its cleavage sequence than to the structural changes that result from supercoiling. EcoRV bends DNA by 55° at the cleavage site (39) and it could plausibly have preferred to bind to supercoiled DNA, which on average is more bent. However, this preference, if it exists, is dwarfed by the sequence preference and very strong overall binding affinity ($K_{\text{d}} = 3.7$ pM (26)), and we did not observe any evidence of topology-dependent binding affinity.

Tfam binding affinities were measured relative to $\Delta L_{\text{k}} = -1$ because the nicked band was indistinguishable from the $\Delta L_{\text{k}} = 0$ band. Tfam negatively supercoils DNA (40) and also imposes a sharp, nearly 180° bend in DNA (22,41) upon binding. Therefore, it is unsurprising that Tfam binds more strongly to supercoiled rather than to relaxed DNA. Negatively supercoiled DNA is more likely to contain preformed bends at the apical ends of plectonemes relative to relaxed DNA. Tfam displayed greater topology-dependent
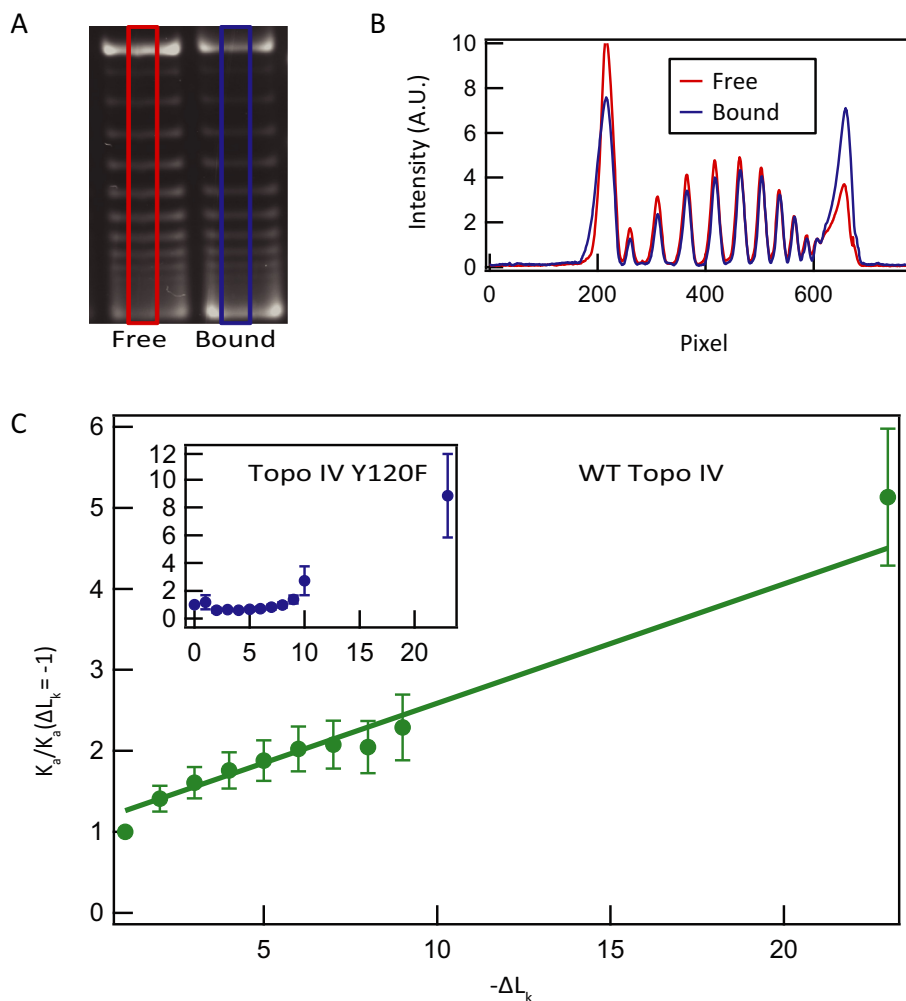
Figure 2. Topology-dependent binding of Topoisomerase IV to pBR322. (A) Unbound and Topo IV-bound DNA visualized by SYBR Green staining after electrophoresis in a 1% agarose gel. The sharpest central parts of the gel lanes were quantified to maximize the resolution (blue and red boxes). (B) Free (red) and Topo IV-bound (blue) DNA from densitometry scans of the gel in A plotted as intensity per pixel. The free DNA distribution has relatively more DNA at lower linking numbers, whereas the bound DNA distribution has relatively more DNA at higher linking numbers. (C) Relative K_a as a function of the plasmid linking number ΔL_k. K_a ratios were calculated for DNA topoisomers bound by Topo IV (Equation 3), normalized to the affinity for the topoisomer $\Delta L_k = -1$ (green dots; error bars represent the standard error of four measurements) and fit to a line (K_a ratio $= 1.12 + 0.15(-\Delta L_k)$; $\chi^2 = 1.49$). Inset, relative K_a as a function of the plasmid linking number ΔL_k for Topo IV with an active site mutation Y120F (error bars represent the standard error of four measurements).

binding for highly negatively supercoiled versus relaxed DNA than did either Topo I or EcoRV.

All of the proteins tested with the exception of EcoRV had higher affinities for negatively supercoiled over relaxed DNA. It may be that a higher binding affinity for supercoiled DNA is a general property of DNA binding proteins rather than one that is specific to individual proteins. Nevertheless, the degree of topology-dependent binding and the precise relationship between supercoiling and affinity varies among the enzymes tested. Topo IV, a protein whose activity depends on the topological state of its substrate, has the highest level of topology-dependent binding of all the proteins tested, whereas EcoRV, whose activity is dependent on a particular DNA sequence rather than on DNA topology, displayed no significant dependence of binding affinity on supercoiling.

Extending the range of measured K_a values

Because the resolution limits of agarose gels prevent the quantification of individual topoisomers with more than ∼10 supercoils, we attempted to use 2D gels to obtain the full range of topoisomers. However, we were unable to obtain individual topoisomer resolution with this method (data not shown). Nevertheless, we were able to take advantage of the fact that plasmid DNA *in vivo* contains a distribution of topoisomers to obtain individual topoisomer resolution for highly supercoiled pBR322 plasmids.

Tfam binding affinities were measured with pBR322 plasmid as purified. The agarose gel and buffer contained 3.5 µg/ml chloroquine, a DNA intercalating agent that induces positive DNA supercoiling and alters the migration of closed circular DNA molecules. The chloroquine decreased the migration rates of highly negatively supercoiled topoisomers making them separable on an agarose gel. The level
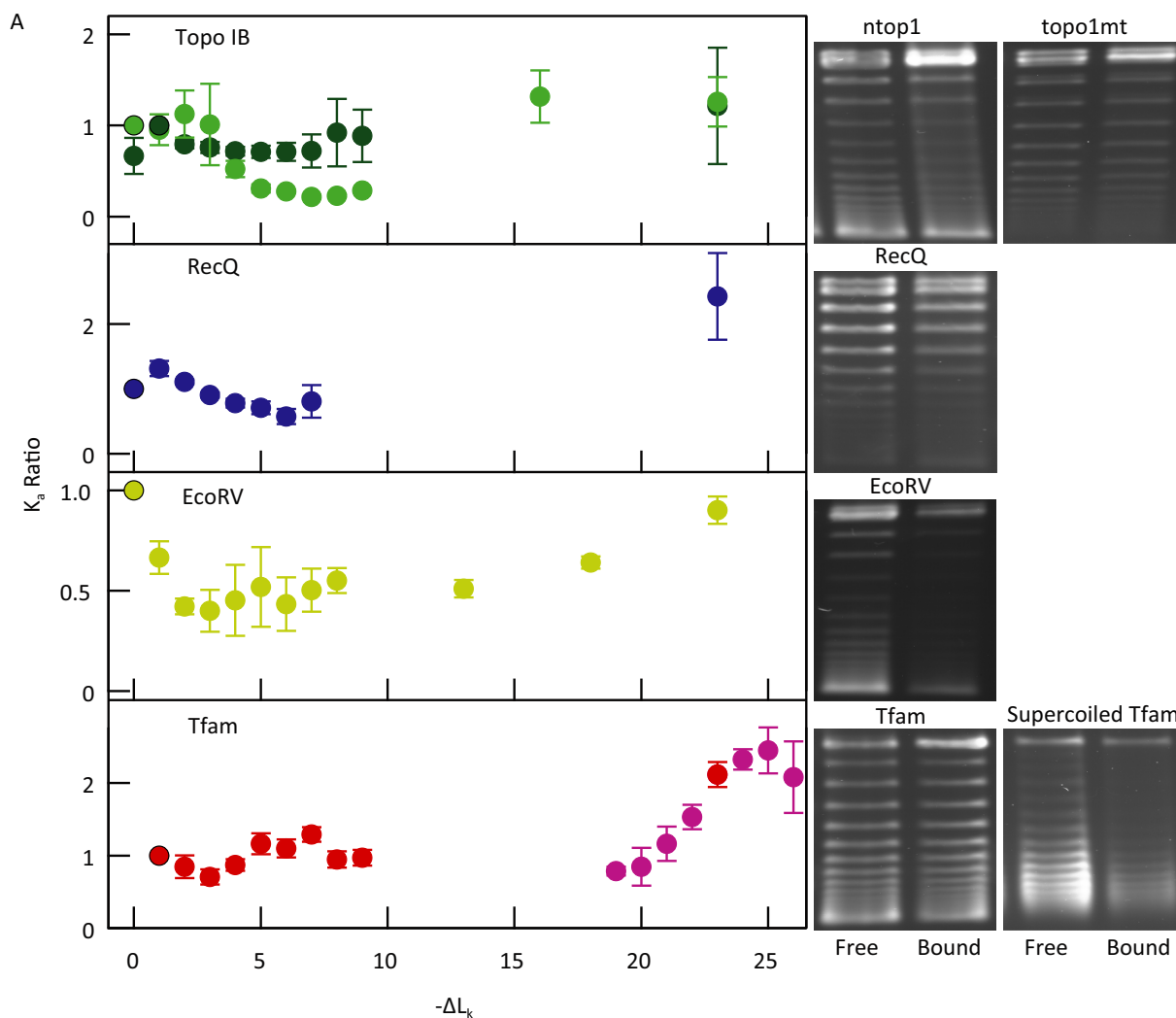
Protein	K_{aN}/K_{a0}	K_{aS}/K_{a0}
ntop1	8.6 ± 3.3	1.3 ± 0.3
RecQ	2.5 ± 0.3	2.4 ± 0.7
EcoRV	0.8 ± 0.1	0.9 ± 0.1
*Tfam	1.4 ± 0.3	0.9 ± 0.2

*Indicates Ka1 used in place of Ka0

Figure 3. (A) Relative binding affinities (K_a) normalized to the affinity for topoisomer $\Delta L_k = 0$ (ntop1, light green; top1mt, dark green; RecQ, blue; EcoRV, yellow) or to the affinity for topoisomer $\Delta L_k = -1$ (Tfam, red; pink). The undifferentiated band was assigned a value of $\Delta L_k = -23$ as an estimate of the expected value of the unresolvable band containing all topoisomers with ΔL_k values below -10. Other Gaussians fit to bands not clearly separable as individual topoisomers were assigned intermediate values. Pink circles represent the results of a Tfam binding experiment using supercoiled pBR322, and were normalized to the empirically determined relative K_a value for $\Delta L_k = -23$. The data points to which the data were normalized are ringed by black circles and error bars represent the standard error of at least four experiments. The gel images to the right of each protein contain unenhanced images of agarose gels containing unbound (left column) and bound (right column) pBR322 topoisomer distributions. In each case the topmost band contains nicked DNA, followed by topoisomers in order of decreasing ΔL_k. The bottommost image contains supercoiled DNA for the higher topoisomer range Tfam binding experiment and was electrophoresed in the presence of 3.5 μg/ml chloroquine. (B) Table of relative binding affinities for nicked plasmids (K_{aN}/K_{a0}) and for highly supercoiled ($\Delta L_k = -23$) plasmids (K_{aS}/K_{a0}).

of chloroquine was selected to maximize the separation of highly supercoiled topoisomers. The most abundant topoisomer was assigned a value of $\Delta L_k = -25$, which corresponds to 6% negative supercoiling for the 4361 bp pBR322 plasmid. Relative K_a values were determined for topoisomers with $-\Delta L_k$ values between 19 and 26, which, together with the data near the origin, provides a more complete Tfam binding affinity profile. Tfam binding affinity varies very little at low supercoiling values and then increases sharply for $-\Delta L_k$ values above 20 (Figure 3).

DISCUSSION

Although DNA topology is known to have a profound impact on protein activity and cellular processes, many protein-DNA interaction measurements employ linear DNA substrates. Current methods to study DNA-protein binding of supercoiled substrates can be laborious, compare only two substrates at once and are often out of equilibrium. The modified nitrocellulose binding assay combined with agarose gel electrophoresis that we developed can measure the relative binding affinity of a protein to ~10 DNA topological forms simultaneously, principally limited by the ability to resolve and quantify topoisomers. This topology-dependent binding assay is generalizable to any DNA-binding protein that can be captured on a nitrocellulose filter and any DNA topologies that can be distinguished by gel electrophoresis. By design the assay is largely insensitive to variances in gel loading, staining or total DNA or protein concentration. When combined with techniques for measuring absolute binding affinity it can create a more complete picture of how proteins may interact with DNA *in vivo*.

Increased affinity for more highly supercoiled DNA is a property that is shared by most of the tested enzymes despite their differences in structure, function and cellular compartment. The only exception is the sequence-dependent restriction enzyme EcoRV. The energetic costs of bending DNA decrease as the DNA is supercoiled and many proteins induce a bend upon binding (15). The broad preference for supercoiled DNA, while generally modest, suggests that the proteins evolved to interact with DNA as it is found *in vivo*. It would be enlightening to test DNA-binding proteins from species whose genetic material is not negatively supercoiled to determine whether they have evolved to interact more strongly with their own native substrates. For example, a range of DNA topologies including the native positively supercoiled form (42) could be tested with DNA binding proteins isolated from a hyperthermophile. Similarly, measurements of relative affinity for positively and negatively supercoiled DNA would shed light on chiral binding discrimination and would provide a means of discerning the differential effects of twist and writhe on protein binding.

The resolution limit of separating pBR322 topoisomers on an agarose gel was partially overcome in the case of Tfam by using a second substrate containing a smaller range of highly supercoiled topoisomers and performing the electrophoresis in the presence of chloroquine, allowing us to obtain K_a ratios for values of ΔL_k between −19 and −26. This approach is relatively straightforward and can be used

to obtain values for substrates in the physiological supercoiling range ($\sigma = -0.06$). In theory, a substrate could be generated containing intermediate values of ΔL_k between −10 and −20 to fill in the remaining gap in the data. For example, it is possible to generate intermediate linking numbers by adding DNA intercalating agents, such as ethidium bromide, while relaxing DNA with a topoisomerase (43). Separating topoisomers on agarose gels in the presence of varying levels of chloroquine can also distinguish between topoisomers with positive and negative supercoils that migrate at the same rate in the absence of an intercalating agent. Another approach to access additional topoisomer values simultaneously is 2D gels with the first dimension run in the absence and the second in the presence of chloroquine. We attempted this but were unable to achieve sufficient resolution to resolve topoisomers with high linking numbers.

One limitation is that the topology-dependent binding assay described here only works for proteins that bind to nitrocellulose, which is not a universal property (44). However, other types of affinity columns such as those that trap His- or other-tagged proteins could be used to obtain relative binding information for proteins that do not bind to nitrocellulose. Finally, an estimate of the absolute value of K_d is helpful to determine appropriate DNA and protein concentrations in the binding reaction. Nevertheless, the relative affinity can be measured accurately even without the knowledge of the K_d because the relative binding affinity measurements can be repeated at successively lower protein concentrations. At concentrations below which the probability of multiple proteins binding to a plasmid falls below $\sim 5\%$, the relative affinity measurements will not depend on the absolute concentration of protein. This procedure can be applied to extract the relative affinity for DNA topoisomers and an estimate of the overall K_d for DNA.

In summary, we have developed a robust and easily implemented DNA topology-dependent protein binding assay. When combined with other data, it may yield insights into the mechanism and function of a variety of DNA-binding proteins across many classes. In addition, the assay can help determine what physical aspects of DNA render proteins sensitive to DNA topology. These could include twist, which influences the melting probability, and writhe, which influences DNA juxtaposition probability and the energetics of bending. DNA distortions may also play a role.

REFERENCES

1. Delbrück,M. (1954) On the replication of desoxyribonucleic acid (DNA). *Proc. Natl. Acad. Sci. U.S.A.*, **40**, 783–788.
2. Liu,L.F. and Wang,J.C. (1987) Supercoiling of the DNA template during transcription. *Proc. Natl. Acad. Sci. U.S.A.*, **84**, 7024–7027.
3. Wang,J.C. (2002) Cellular roles of DNA topoisomerases: a molecular perspective. *Nat. Rev. Mol. Cell. Biol.*, **3**, 430–440.
4. Schvartzman,J.B. and Stasiak,A. (2004) A topological view of the replicon. *EMBO Rep.*, **5**, 256–261.
5. Wasserman,S.A. and Cozzarelli,N.R. (1986) Biochemical topology: applications to DNA recombination and replication. *Science*, **232**, 951–960.
6. Downes,C.S., Clarke,D.J., Mullinger,A.M., Giménez-Abián,J.F., Creighton,A.M. and Johnson,R.T. (1994) A topoisomerase II-dependent G2 cycle checkpoint in mammalian cells. *Nature*, **372**, 467–470.
7. Sumners,D.W., Ernst,C., Spengler,S.J. and Cozzarelli,N.R. (1995) Analysis of the mechanism of DNA recombination using tangles. *Q. Rev. Biophys.*, **28**, 253–313.
8. Vinograd,J., Lebowitz,J., Radloff,R., Watson,R. and Laipis,P. (1965) The twisted circular form of polyoma viral DNA. *Proc. Natl. Acad. Sci. U.S.A.*, **53**, 1104–1111.
9. Cozzarelli,N.R. (1980) DNA gyrase and the supercoiling of DNA. *Science*, **207**, 953–960.
10. Worcel,A. and Burgi,E. (1972) On the structure of the folded chromosome of Escherichia coli. *J. Mol. Biol.*, **71**, 127–147.
11. Vologodskii,A.V. and Cozzarelli,N.R. (1994) Conformational and thermodynamic properties of supercoiled DNA. *Annu. Rev. Biophys. Biomol. Struct.*, **23**, 609–643.
12. Vologodskii,A.V., Levene,S.D., Klenin,K.V., Frank-Kamenetskii,M. and Cozzarelli,N.R. (1992) Conformational and thermodynamic properties of supercoiled DNA. *J. Mol. Biol.*, **227**, 1224–1243.
13. Fogg,J.M., Randall,G.L., Pettitt,B.M., Sumners,d.W., Harris,S.A. and Zechiedrich,L. (2012) Bullied no more: when and how DNA shoves proteins around. *Q. Rev. Biophys.*, **45**, 257–299.
14. Wei,J., Czapla,L., Grosner,M.A., Swigon,D. and Olson,W.K. (2014) DNA topology confers sequence specificity to nonspecific architectural proteins. *Proc. Natl. Acad. Sci. U.S.A.*, **111**, 16742–16747.
15. Rohs,R., Jin,X., West,S.M., Joshi,R., Honig,B. and Mann,R.S. (2010) Origins of specificity in protein-DNA recognition. *Annu. Rev. Biochem.*, **79**, 233–269.
16. Madden,K.R., Stewart,L. and Champoux,J.J. (1995) Preferential binding of human topoisomerase I to superhelical DNA. *EMBO J.*, **14**, 5399–5409.
17. Martínez-García,B., Fernández,X., Díaz-Ingelmo,O., Rodríguez-Campos,A., Manichanh,C. and Roca,J. (2013) Topoisomerase II minimizes DNA entanglements by proofreading DNA topology after DNA strand passage. *Nucleic Acids Res*, **42**, 1821–1830.
18. Stone,M.D., Bryant,Z., Crisona,N.J., Smith,S.B., Vologodskii,A., Bustamante,C. and Cozzarelli,N.R. (2003) Chirality sensing by Escherichia coli topoisomerase IV and the mechanism of type II topoisomerases. *Proc. Natl. Acad. Sci. U.S.A.*, **100**, 8654–8659.
19. Remus,D., Beall,E.L. and Botchan,M.R. (2004) DNA topology, not DNA sequence, is a critical determinant for Drosophila ORC-DNA binding. *EMBO J.*, **23**, 897–907.
20. Roca,J. (2001) Filter binding assays for topoisomerase-DNA complexes. *Methods Mol. Biol.*, **95**, 75–80.
21. Clore,G.M., Gronenborn,A.M. and Davies,R.W. (1982) Theoretical aspects of specific and non-specific equilibrium binding of proteins to DNA as studied by the nitrocellulose filter binding assay. Co-operative and non-co-operative binding to a one-dimensional lattice. *J. Mol. Biol.*, **155**, 447–466.
22. Rubio-Cosials,A., Sidow,J.F., Jimenez-Menendez,N., Fernandez-Millan,P., Montoya,J., Jacobs,H.T., Coll,M., Bernado,P. and Sola,M. (2011) Human mitochondrial transcription factor A induces a U-turn structure in the light strand promoter. *Nat. Struct. Mol. Biol.*, **18**, 1281–1289.
23. Tropea,J.E., Cherry,S. and Waugh,D.S. (2009) Expression and purification of soluble His(6)-tagged TEV protease. *Methods Mol. Biol.*, **498**, 297–307.
24. Corbett,K.D., Schoeffler,A.J., Thomsen,N.D. and Berger,J.M. (2005) The structural basis for substrate specificity in DNA topoisomerase IV. *J. Mol. Biol.*, **351**, 545–561.
25. Hardin,A.H., Sarkar,S.K., Seol,Y., Liou,G.F., Osheroff,N. and Neuman,K.C. (2011) Direct measurement of DNA bending by type IIA topoisomerases: implications for non-equilibrium topology simplification. *Nucleic Acids Res.*, **39**, 5729–5743.
26. Hiller,D.A., Fogg,J.M., Martin,A.M., Beechem,J.M., Reich,N.O. and Perona,J.J. (2003) Simultaneous DNA binding and bending by EcoRV endonuclease observed by real-time fluorescence. *Biochemistry*, **42**, 14375–14385.
27. Farge,G., Laurens,N., Broekmans,O.D., van den Wildenberg,S.M., Dekker,L.C., Gaspari,M., Gustafsson,C.M., Peterman,E.J., Falkenberg,M. and Wuite,G.J. (2012) Protein sliding and DNA denaturation are essential for DNA organization by human mitochondrial transcription factor A. *Nat. Commun.*, **3**, 1013.
28. Madden,K.R. and Champoux,J.J. (1992) Overexpression of human topoisomerase I in baby hamster kidney cells: hypersensitivity of clonal isolates to camptothecin. *Cancer Res.*, **52**, 525–532.
29. Mo,Y.Y., Wang,P. and Beck,W.T. (2000) Functional expression of human DNA topoisomerase I and its subcellular localization in HeLa cells. *Exp. Cell. Res.*, **256**, 480–490.
30. Lin,C.H., Chen,Y.C. and Pan,T.M. (2011) Quantification bias caused by plasmid DNA conformation in quantitative real-time PCR assay. *PLoS ONE*, **6**, e29101.
31. Peng,H. and Marians,K.J. (1995) The interaction of Escherichia coli topoisomerase IV with DNA. *J. Biol. Chem.*, **270**, 25286–25290.
32. Anderson,V.E., Gootz,T.D. and Osheroff,N. (1998) Topoisomerase IV catalysis and the mechanism of quinolone action. *J. Biol. Chem.*, **273**, 17879–17885.
33. Dong,K.C. and Berger,J.M. (2007) Structural basis for gate-DNA recognition and bending by type IIA topoisomerases. *Nature*, **450**, 1201–1205.
34. Champoux,J.J. (1981) DNA is linked to the rat liver DNA nicking-closing enzyme by a phosphodiester bond to tyrosine. *J. Biol. Chem.*, **256**, 4805–4809.
35. Lebedeva,N., Auffret Vander Kemp,P., Bjornsti,M.A., Lavrik,O. and Boiteux,S. (2006) Trapping of DNA topoisomerase I on nick-containing DNA in cell free extracts of Saccharomyces cerevisiae. *DNA Repair (Amst)*, **5**, 799–809.
36. Muller,M.T. (1985) Quantitation of eukaryotic topoisomerase I reactivity with DNA. Preferential cleavage of supercoiled DNA. *Biochim. Biophys. Acta*, **824**, 263–267.
37. Zhang,H., Barceló,J.M., Lee,B., Kohlhagen,G., Zimonjic,D.B., Popescu,N.C. and Pommier,Y. (2001) Human mitochondrial topoisomerase I. *Proc. Natl. Acad. Sci. U.S.A.*, **98**, 10608–10613.
38. Moreno-Herrero,F., Holtzer,L., Koster,D.A., Shuman,S., Dekker,C. and Dekker,N.H. (2005) Atomic force microscopy shows that vaccinia topoisomerase IB generates filaments on DNA in a cooperative fashion. *Nucleic Acids Res.*, **33**, 5945–5953.
39. Perona,J.J. and Martin,A.M. (1997) Conformational transitions and structural deformability of EcoRV endonuclease revealed by crystallographic analysis. *J. Mol. Biol.*, **273**, 207–225.
40. Fisher,R.P., Lisowsky,T., Parisi,M.A. and Clayton,D.A. (1992) DNA wrapping and bending by a mitochondrial high mobility group-like transcriptional activator protein. *J. Biol. Chem.*, **267**, 3358–3367.
41. Ngo,H.B., Kaiser,J.T. and Chan,D.C. (2011) The mitochondrial transcription and packaging factor Tfam imposes a U-turn on mitochondrial DNA. *Nat. Struct. Mol. Biol*, **18**, 1290–1296.

42. Forterre,P., Bergerat,A. and Lopez-Garcia,P. (1996) The unique DNA topology and DNA topoisomerases of hyperthermophilic archaea. *FEMS Microbiol. Rev.*, **18**, 237–248.

43. Keller,W. (1975) Determination of the number of superhelical turns in simian virus 40 DNA by gel electrophoresis. *Proc. Natl. Acad. Sci. U.S.A.*, **72**, 4876–4880.

44. Oehler,S., Alex,R. and Barker,A. (1999) Is nitrocellulose filter binding really a universal assay for protein-DNA interactions? *Anal. Biochem.*, **268**, 330–336.